9th IEEE-RAS International Conference on Humanoid Robots
December 7-10, 2009 Paris, France

Solvability-unconcerned Inverse Kinematics based on Levenberg-Marquardt method with Robust Damping

Tomomichi Sugihara
School of Information Science and Electrical Engineering, Kyushu University
744 Moto'oka, Nishi-ku, Fukuoka, Japan
zhidao@ieee.org

***Abstract*— A robust numerical solution to the inverse kinematics is presented based on Levenberg-Marquardt method. The equation solvability in addition to the singularity doesn't concern the method; even in cases where the problem doesn't have solutions or has countless solutions, it converges to the optimum solution in the sense that it minimizes the residual from the target points with the smallest joint deviations. The squared norm of the residual with a small bias is used for the damping factor, while its numerical stability, convergence performance and computation speed are remarkable. It is suitable to large-scale structure-varying kinematic chains, in which the relationship between the number of constraints and the degree-of-freedom frequently changes. It frees robot operators from being careful about the assignment of the target points of effectors. As an application of the proposed method, a stretched-knee walking motion of a humanoid robot is designed.**

***Index Terms*— Inverse kinematics, Levenberg-Marquardt method, Numerical robustness, Humanoid robot.**

I. INTRODUCTION

Inverse kinematics (IK), in which the joint displacements are computed to achieve the targeted position and orientation of effectors, is one of the fundamental, yet difficult computations in robotics. As Pieper[1] showed, it comes down to solving simultaneous high-order polynomial equations. Except for particular well-studied classes of manipulators [1][2],analytical solutions are not available in general cases, and hence numerical solutions are often required.

Newton-Raphson method (**NR**) is a frequently used technique in this regard. An efficient computation of manipulator Jacobian matrix to be used in this method was presented[3].It is known, however, that NR doesn't guarantee the global convergence so that it is sensitive to the initial value. In addition, the following properties underlying in IK makes the problem more awkward.

1) The equation solvability is not necessarily guaranteed; it is difficult to know if the targeted position and orientation of effectors are kinematically acceptable before trying to solve IK.
2) The number of independent equations doesn't necessarily coincide with the degree-of-freedom, namely, the number of unknowns. If the former is more than the latter, it is called *overconstrained* problem where the equation is unsolvable. If the former is less than the latter, it is called *underconstrained* problem, which happens in cases of redundant robots.
3) Even in cases of non-redundant robots, countless solutions of IK might exist at singular points, where the manipulator Jacobian matrix is not row-fullrank.

The problems of redundancy and singularity have been studied mainly in the differential inverse kinematics (motion rate resolution) [3][4][5][6][7].Whitney[3] suggested the use of Moore-Penrose's pseudoinverse matrix (MP-inverse), which gives a locally-optimized joint deviation at singular points. Nakamura and Hanafusa[5] claimed that it suffered from numerical ill-posedness rather in the vicinity of singular points, and proposed Singularity-robust inverse matrix (SR-inverse). It is identical with the damped least-square method proposed by Wampler[6], which is, as pointed out in the literature, a version of Levenberg-Marquardt method (**LM**)[8].

The problems of overconstraint and unsolvability also have not been sufficiently discussed; they are as crucial as redundancy and singularity problems particularly in cases of large-scale structure-varying[9] kinematic chains such as humanoid robots. It is a burden for motion designers or teleoperators to assign target points carefully within the work space. From this viewpoint, it is reasonable to substitute IK for a minimization of the residual. Wolovich et al.[10] and Balestrino et al.[11] proposed to use Jacobian transpose matrix instead of pseudoinverse. It is mathematically equivalent with steepest descent method (**SD**), which globally converges to a local minimizer. A drawback is that the convergence is linear, namely, very slow. Zhao and Badler[12] proposed to use variable metric (quasi-Newton) method (**VM**) with superlinear convergence. We found that it is often captured at local minima, and thus is not reliable. LM is potentially the most reliable method for minimization. It is known, however, that the success or failure depends on the choice of the damping factor. Though several ideas[5][13][14][15][16] to choose it have been proposed, it is still unclear how to choose it in terms of the convergence performance.

The paper proposes a damping technique on LM to achieve efficient and robust IK against singularity, redundancy, and even unsolvability. The idea is rather simple that the squared norm of the residual with a small bias is used for the damping factor, while it is remarkably stable and fast no matter how far the target point is from the solvable range. It computes the optimal configuration in the sense that it minimizes the residual from the target points. If the problem is solvable, it converges to the solution regardless of redundancy and singularity. Some numerical evaluations on a kinematic model of a redundant manipulator show that it stably converges without a fine initial guess. As an application of the proposed method, a humanoid robot walking motion trajectory with stretched-knee is designed.

*This work is supported by "The Kyushu University Research Superstar Program (SSP)", based on the budget of Kyushu University allocated under President's initiative.

II. MINIMIZATION APPROACH TO IK

Basically, the robot kinematics is mathematically represented by a set of constraints on the joint displacement vector $\boldsymbol{q} = [q_1\ q_2\ \cdots\ q_n]^{\mathrm{T}} \in \mathbb{R}^n$, where n is the degree-of-freedom. A positional constraint is represented as

$$\boldsymbol{p}_i(\boldsymbol{q}) = {}^d\boldsymbol{p}_i, \tag{1}$$

where $\boldsymbol{p}_i \in \mathbb{R}^3$ locates a point of interest in the robot body, and ${}^d\boldsymbol{p}_i \in \mathbb{R}^3$ is the targeted position in the space. Not to mension, they are with respect to the same coordinate frame. For an orientational constraint,

$$\boldsymbol{R}_i(\boldsymbol{q}) = {}^d\boldsymbol{R}_i, \tag{2}$$

where $\boldsymbol{R}_i \in SO(3)$ is for the orientation of a link of interest, and ${}^d\boldsymbol{R}_i \in SO(3)$ is the targeted orientation in the space. In both cases, the residual vector $\boldsymbol{e}_i(\boldsymbol{q})$ can be defined as

$$\boldsymbol{e}_i(\boldsymbol{q}) \equiv \begin{cases} {}^d\boldsymbol{p}_i - \boldsymbol{p}_i(\boldsymbol{q}) & \text{(for a positional constraint)} \\ \boldsymbol{a}({}^d\boldsymbol{R}_i\boldsymbol{R}_i(\boldsymbol{q})^{\mathrm{T}}) & \text{(for an orientational constraint)} \end{cases}, \tag{3}$$

where $\boldsymbol{a}(\boldsymbol{R}) \in \mathbb{R}^3$ for an arbitrary $\boldsymbol{R} \in SO(3)$ is the equivalent angle-axis vector defined in Appendix A. Also, we define the whole residual vector $\boldsymbol{e}(\boldsymbol{q}) \in \mathbb{R}^{3N}$ here as

$$\boldsymbol{e}(\boldsymbol{q}) \equiv \begin{bmatrix} \boldsymbol{e}_1(\boldsymbol{q}) \\ \boldsymbol{e}_2(\boldsymbol{q}) \\ \vdots \\ \boldsymbol{e}_N(\boldsymbol{q}) \end{bmatrix}, \tag{4}$$

where $3N$ is the total number of constraints. Our interest starts from solving the following nonlinear equation:

$$\boldsymbol{e}(\boldsymbol{q}) = \boldsymbol{0}. \tag{5}$$

The conventional IK based on NR tries to find $\boldsymbol{q} = \boldsymbol{q}^*$ which satisfies Eq.(5) by the following update rule:

$$\boldsymbol{q}_{k+1} = \boldsymbol{q}_k - \nabla\boldsymbol{e}(\boldsymbol{q}_k)^{-1}\boldsymbol{e}_k, \tag{6}$$

where $\boldsymbol{e}_k \equiv \boldsymbol{e}(\boldsymbol{q}_k)$. $\nabla\boldsymbol{e}$ is substitutable with the manipulator Jacobian matrix $\boldsymbol{J}(\boldsymbol{q})$ as

$$\nabla\boldsymbol{e}(\boldsymbol{q}_k) \simeq -\boldsymbol{J}_k, \tag{7}$$

where $\boldsymbol{J}_k \equiv \boldsymbol{J}(\boldsymbol{q}_k)$. Implicit assumptions are 1) $n = 3N$, 2) $\boldsymbol{J}_k$ is a regular square matrix, and 3) Eq.(5) is solvable, namely, has at least one solution. If any of them is violated, this iteration computation bankrupts. Also, the initial value $\boldsymbol{q} = \boldsymbol{q}_0$ should be close enough to $\boldsymbol{q}^*$ since NR doesn't guarantee the global convergence.

In order to discuss the global convergence even in unsolvable cases, we focus on the following minimization problem instead of the original equation (5):

$$E(\boldsymbol{q}) \equiv \frac{1}{2}\boldsymbol{e}^{\mathrm{T}}\boldsymbol{W}_e\boldsymbol{e} \to \min. \tag{8}$$

where $\boldsymbol{W}_e = diag\{w_{e,i}\}$ ($w_{e,i} > 0$ for $\forall i = 1 \sim 3N$) is a weighting matrix on the constraints. Note that Eq.(5) and the problem (8) are not equivalent. This translation implies that we give up finding the solution and accept the minimizer as an approximate solution, prioritizing the numerical and practical safety. NR is still available for the problem (8) in a slightly different fashion. From the definition of the evaluation function $E(\boldsymbol{q})$, we get

$$\nabla E = \boldsymbol{e}^{\mathrm{T}}\boldsymbol{W}_e\nabla\boldsymbol{e} \tag{9}$$

$$\nabla^2 E = \nabla\boldsymbol{e}^{\mathrm{T}}\boldsymbol{W}_e\nabla\boldsymbol{e} + \sum_{i=1}^{n}\frac{\partial\nabla\boldsymbol{e}}{\partial q_i}\boldsymbol{W}_e\boldsymbol{e}, \tag{10}$$

where $\frac{\partial\nabla\boldsymbol{e}}{\partial q_i} \simeq -\frac{\partial\boldsymbol{J}}{\partial q_i}$ is related to the manipulator Hessian [17][18][19]. Then, NR for this minimization runs with the following update rule:

$$\boldsymbol{q}_{k+1} = \boldsymbol{q}_k - (\nabla^2 E)^{-1}\nabla E^{\mathrm{T}}. \tag{11}$$

Our objective is, however, to find a descent direction of the evaluation function E rather than to calculate the exact curvature of E. It is preferable to find a positive-definite matrix instead of using $\nabla^2 E$ straightforward in Eq.(11). If the latter term of Eq.(10) is omitted, it is Gauss-Newton method (**GN**) and Eq.(11) turns to

$$\boldsymbol{q}_{k+1} = \boldsymbol{q}_k + (\boldsymbol{J}_k^{\mathrm{T}}\boldsymbol{W}_e\boldsymbol{J}_k)^{-1}\boldsymbol{g}_k \tag{12}$$

$$\boldsymbol{g}_k \equiv \boldsymbol{J}_k^{\mathrm{T}}\boldsymbol{W}_e\boldsymbol{e}_k \tag{13}$$

where Eq.(7) is applied. It is the same with using weighted-norm-minimizing generalized inverse of $\boldsymbol{J}_k$ instead of $\nabla\boldsymbol{e}(\boldsymbol{q}_k)^{-1}$ in Eq.(6). Eq.(13) is valid as long as $\boldsymbol{J}_k$ is non-singular. When this assumption is jeopardized, the problem becomes numerically ill-posed. LM[8] is an alternative to resolve this defect, with which Eq.(13) turns to

$$\boldsymbol{q}_{k+1} = \boldsymbol{q}_k + \boldsymbol{H}_k^{-1}\boldsymbol{g}_k \tag{14}$$

$$\boldsymbol{H}_k \equiv \boldsymbol{J}_k^{\mathrm{T}}\boldsymbol{W}_e\boldsymbol{J}_k + \boldsymbol{W}_n \tag{15}$$

where $\boldsymbol{W}_n = diag\{w_{n,i}\}$ ($w_{n,i} > 0$ for $\forall i = 1 \sim n$) is called the damping factor. Note that $\boldsymbol{H}_k$ is guaranteed to be regular and positive-definite, and thus the incremental term in Eq.(15) necessarily faces a descent direction. One can regard it as the simplest form of Tikhonov's regularization[20]. As Nakamura and Hanafusa[5] pointed out, Eq.(15) is also equivalent with solving the following mixed minimization problem at each iteration step:

$$\frac{1}{2}\boldsymbol{r}_k^{\mathrm{T}}\boldsymbol{W}_e\boldsymbol{r}_k + \frac{1}{2}\Delta\boldsymbol{q}_k^{\mathrm{T}}\boldsymbol{W}_n\Delta\boldsymbol{q}_k \to \min. \tag{16}$$

where $\Delta\boldsymbol{q}_k \equiv \boldsymbol{q}_{k+1} - \boldsymbol{q}_k$ and $\boldsymbol{r}_k \equiv \boldsymbol{e}_k - \boldsymbol{J}_k\Delta\boldsymbol{q}_k$, so that it converges to a certain configuration with the minimum joint deviations even in cases of redundant robots.

III. SOLVABILITY-UNCONCERNED IK

Although many ideas[5][13][14][15][16] have been proposed on the choice of $\boldsymbol{W}_n$, it has been rarely discussed from the viewpoint of convergence performance. Only Chan and Lawrence[13] investigated the iteration process and proposed the error damped pseudoinverse, which defines:

$$\boldsymbol{W}_n = E_k\boldsymbol{1} \tag{17}$$

where $E_k \equiv E(\boldsymbol{q}_k)$ and $\boldsymbol{1}$ is $n \times n$ identity matrix. Since E_k quadratically converges to zero as $\boldsymbol{q}_k$ converges to the solution, the iteration is expected to be superlinear convergence. If the solution is close to the singular point, however,

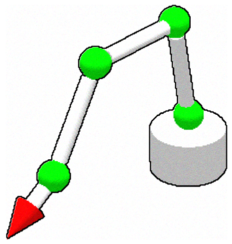

Fig. 1. Kinematics model of the tested manipulator with four links and spherical joints.

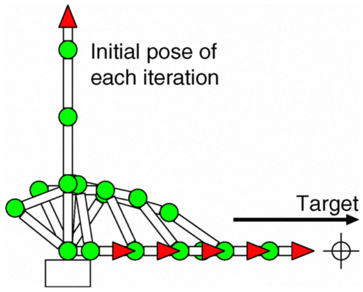

Fig. 2. In the first test, the target position of the endpoint is moved from 0.1 to 1.0[m] step-by-step.

the coefficient matrix would become ill-conditioned. Our method is rather simple, which defines $\boldsymbol{W}_n$ as

$$\boldsymbol{W}_n = E_k \boldsymbol{1} + \overline{\boldsymbol{W}}_n \tag{18}$$

where $\overline{\boldsymbol{W}}_n = diag\{\overline{w}_{n,i}\}$ ($\overline{w}_{n,i} > 0$ for $\forall i = 1 \sim n$) is a small constant bias. Suppose $\overline{\boldsymbol{W}}_n = \overline{w}_n \boldsymbol{1}$ for simplicity, and the singular value decomposition of $\boldsymbol{W}_e^{1/2} \boldsymbol{J}_k$ is

$$\boldsymbol{W}_e^{1/2} \boldsymbol{J}_k = \boldsymbol{U} \boldsymbol{\Sigma} \boldsymbol{V}^{\mathrm{T}}, \tag{19}$$

where $\boldsymbol{U}$ and $\boldsymbol{V}$ are orthonormal, and $\boldsymbol{\Sigma} = diag\{\sigma_i\}$ is a diagonal matrix in which the singular values are arrayed in descending order i.e. $\sigma_1 \geq \sigma_2 \geq \cdots \geq \sigma_n$. Then, we get

$$\begin{aligned} \boldsymbol{H}_k &= \boldsymbol{V} \boldsymbol{\Sigma} \boldsymbol{U}^{\mathrm{T}} \boldsymbol{U} \boldsymbol{\Sigma} \boldsymbol{V}^{\mathrm{T}} + (E_k + \overline{w}_n) \boldsymbol{1} \\ &= \boldsymbol{V} \left\{ \boldsymbol{\Sigma}^2 + (E_k + \overline{w}_n) \boldsymbol{1} \right\} \boldsymbol{V}^{\mathrm{T}}. \end{aligned} \tag{20}$$

The condition number κ of this matrix is

$$\kappa = \|\boldsymbol{H}_k\| \cdot \|\boldsymbol{H}_k^{-1}\| = \frac{\sigma_1^2 + E_k + \overline{w}_n}{\sigma_n^2 + E_k + \overline{w}_n}. \tag{21}$$

Here are some qualitative discussions.

I) If Eq.(5) is solvable and the solution is far from singular points, $\boldsymbol{W}_n$ quadratically converges to $\overline{\boldsymbol{W}}_n$, and thus the iteration is superlinearly convergent[21].

II) If the original Eq.(5) is solvable but the solution is near a singular point, κ approaches to $\dfrac{\sigma_1^2 + \overline{w}_n}{\overline{w}_n}$. Hence, $\overline{w}_n$ is necessary to avoid degeneracy of $\boldsymbol{H}_k$. Although it is a problem how large $\overline{w}_n$ should be, it is not crucial since $\boldsymbol{g}_k \simeq \boldsymbol{0}$ near the solution. In our experiments, $\overline{w}_n = 1.0 \times 10^{-3}$ worked well in any cases.

III) If the original Eq.(5) is unsolvable, κ gets closer to 1 as $\boldsymbol{e}_k$ increases. Namely, the magnitude of the incremental vector $\boldsymbol{H}_k^{-1} \boldsymbol{g}_k$ becomes smaller since $\|\boldsymbol{H}_k^{-1} \boldsymbol{g}_k\| \simeq \dfrac{1}{\|\boldsymbol{e}_k\|}$.

In order to guarantee the global convergence, it should be combined with a line search algorithm such as Moré-Thuente method[22]. However, we empirically found that it succeeded to converge to the global minimum rather without line search as shown in the following section.

IV. Evaluation

A. Evaluation of computation stability and time

The proposed method was evaluated on a redundant manipulator, the kinematics model of which is shown in Fig.1. It comprises four links which are serially connected by four spherical joints. Thus, the manipulator has 12 DOFs. The lengths of the three links from the root are all 0.15[m], while the end-effector's length is 0.05[m].

For comparison, the following methods were also tested:

- SD:steepest descent method†,
- GN:Gauss-Newton method with weighted MP-inverse*,
- LM(λ =const.):Levenberg-Marquardt method with fixed $\boldsymbol{W}_n = \lambda \boldsymbol{1}$,
- LM(NH):Levenberg-Marquardt method with Nakamura-Hanafusa method[5]‡,
- LM(CL):Levenberg-Marquardt method with Chan-Lawrence method,
- LM(proposed):Levenberg-Marquardt method with the proposed damping method,
- LM(MWM):Levenberg-Marquardt method with Mayorga-Wong-Milano method[15]‡,
- LM(Chi):Levenberg-Marquardt method with Chiaverini method[14]‡,
- VM:variable metric method based on BFGS formula without line search, and
- VM(MT):variable metric method based on BFGS formula with Moré-Thuente method.

*GN was implemented by utilizing LQ decomposition, which is faster than the singular value decomposition.

† The iteration in SD is ruled by

$$\boldsymbol{q}_{k+1} = \boldsymbol{q}_k - \frac{E_k}{\boldsymbol{g}_k^{\mathrm{T}} \boldsymbol{g}_k} \boldsymbol{g}_k, \tag{22}$$

which approximates the evaluation function by a quadratic curve.

‡Nakamura-Hanafusa method, Mayorga-Milano-Wong method and Chiaverini method have some parameters, the way to choose which is not trivial. In our tests, they were manually tuned to acquire the best results in terms of both the computation accuracy and time through trials-and-errors; better values were hardly found.

In all iterations, the initial value was set for $\boldsymbol{q}_0 = [0\ 0\ 0\ 0\ 0\ 0]^{\mathrm{T}}$ — note that it is a singular point of the manipulator, and $\boldsymbol{W}_e$ was fixed for $\boldsymbol{1}$. The iteration was terminated in any of the following three cases:

1) every components of incrementing vector $\Delta \boldsymbol{q}_k$ are less than $\epsilon = 1.0 \times 10^{-12}$,
2) the deviation of $\|\boldsymbol{e}_k\|$ from the previous $\|\boldsymbol{e}_{k-1}\|$ is less than $\delta = 1.0 \times 10^{-12}$, or
3) the number of iteration exceeds the limit= 10000.

The target position of the endpoint is set at

$${}^d\boldsymbol{p} = \begin{bmatrix} x_d \\ 0 \\ 0 \end{bmatrix}, \quad {}^d\boldsymbol{R} = \begin{bmatrix} 0 & 0 & 1 \\ 0 & 1 & 0 \\ -1 & 0 & 0 \end{bmatrix}, \tag{23}$$

where x_d is changed from 0.1 to 1.0. Since the manipulator's reach is about 0.5[m], IK becomes unsolvable when $x_d > 0.5$, so that the residual linearly increases with respect to x_d over 0.5 in successful cases. The computational error and time of SD, GN, LM($\lambda = 0.001, 0.01, 0.1$), LM(NH), LM(CL), LM(proposed), LM(MWM), LM(Chi), VM and VM(MT) were compared in Fig.3 and Fig.4, respectively. The dotted lines in Fig.3 shows the minimum solutions. SD, GN, LM(λ =const.), LM(NH), LM(MWM) and LM(Chi) frequently failed to result in the minimum solutions in unsolvable cases. Though VM seems rather successful, the results of it randomly diverged in some cases, so that the method is less reliable. All results of VM(MT) were rapidly captured at local minima. Only LM(CL) and LM(proposed) converged to the minimum in all cases here.

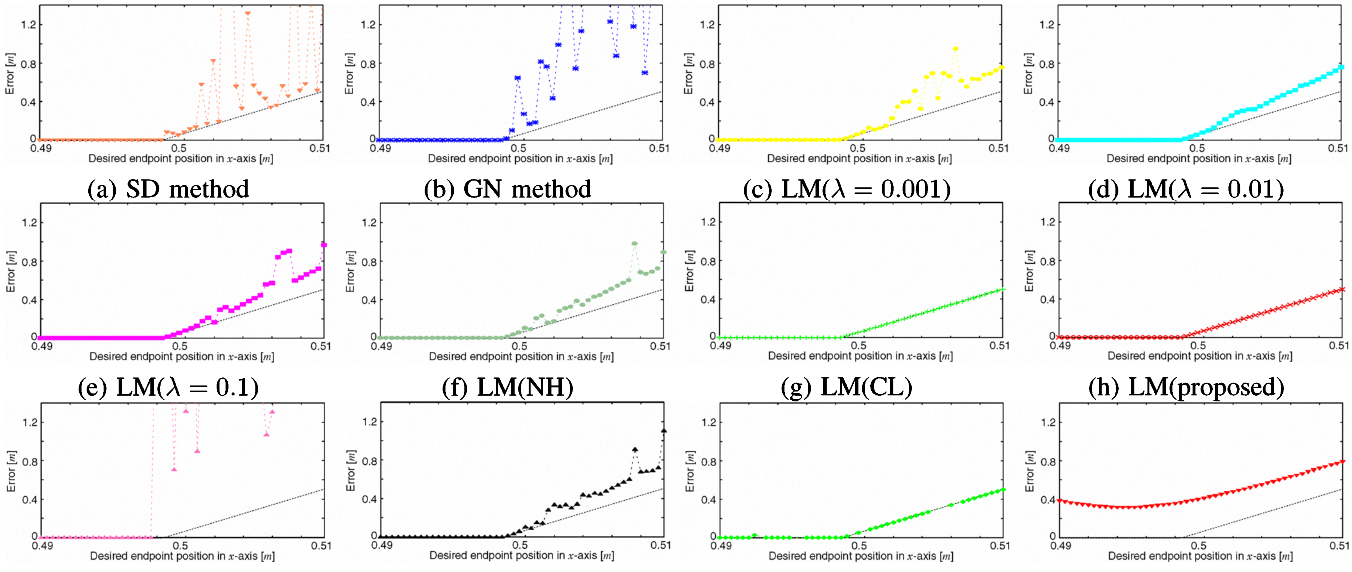

(a) SD method (b) GN method (c) LM($\lambda = 0.001$) (d) LM($\lambda = 0.01$)
(e) LM($\lambda = 0.1$) (f) LM(NH) (g) LM(CL) (h) LM(proposed)
(i) LM(MWM) (j) LM(Chi) (k) VM (l) VM(MT)

Fig. 3. Error comparison between SD, GN, LM(λ =const.), LM(NH), LM(CL), LM(proposed), LM(MWM), LM(Chi), VM and VM(MT). Except for LM(CL) and LM(proposed), all methods failed to achive the minimum solution particularly in unsolvable range. VM made the results diverged in some cases. All results were captured at local minimum by VM(MT).

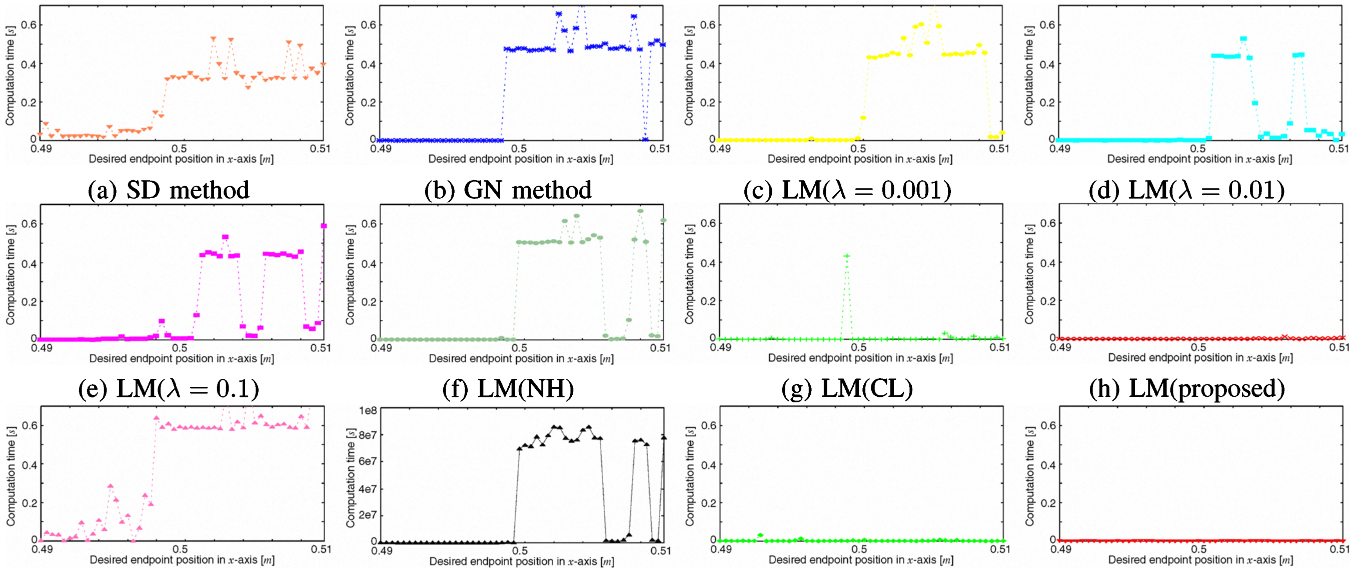

(a) SD method (b) GN method (c) LM($\lambda = 0.001$) (d) LM($\lambda = 0.01$)
(e) LM($\lambda = 0.1$) (f) LM(NH) (g) LM(CL) (h) LM(proposed)
(i) LM(MWM) (j) LM(Chi) (k) VM (l) VM(MT)

Fig. 4. Computation time comparison between SD, GN, LM(λ =const.), LM(NH), LM(CL), LM(proposed), LM(MWM), LM(Chi), VM and VM(MT). Except for the proposed method, all methods failed to terminate iterations in some cases. Particularly, LM(Chi) consumed incomparably long time. Though the result of VM(MT) seems successful, the computations are failed. Refer the caption of Fig.3.

The vicinity of the boundary of the solvable range in Fig.3 and Fig.4 are magnified in Fig.5 and Fig.6, respectively. While LM(λ =const.), LM(NH), LM(Chi) and the proposed method showed stable behaviors even around the boundary, LM(CL) becomes unstable as predicted. Though the proposed method took a long time exactly at the boundary, the iteration stably converged to the solution. Also, any other methods didn't show better performances than the proposed method from the viewpoint of the computation time.

The above results tell that only the proposed method was practically available in the tested cases.

B. *Stretched-knee walk by a humanoid robot*

For an application of the proposed solvability-unconcerned IK, a four-step stretched-knee walk motion by a humanoid robot was planned. For a robot model,

TABLE I

LIST OF POINTS OF INTEREST IN IK.

Point	$(w_{e,x},\ w_{e,y},\ w_{e,z})$
COM	(1.0, 1.0, 0.1)
Body attitude	(1.0, 1.0, 1.0)
Outer toe of left foot	(1.0, 1.0, 1.0)
Inner toe of left foot	(1.0, 1.0, 1.0)
Outer heel of left foot	(0.1, 1.0, 0.001)
Inner heel of left foot	(0.1, 1.0, 0.001)
Outer toe of right foot	(1.0, 1.0, 1.0)
Inner toe of right foot	(1.0, 1.0, 1.0)
Outer heel of right foot	(0.1, 1.0, 0.001)
Inner heel of right foot	(0.1, 1.0, 0.001)

mighty[23] was supposed. The trajectories of the center of mass (COM), the zero-moment point and feet were simultaneously planned based on the boundary condition relaxation method[24]. Particularly, the height of COM was planned to be constant at 0.28[m]. Since the height of the

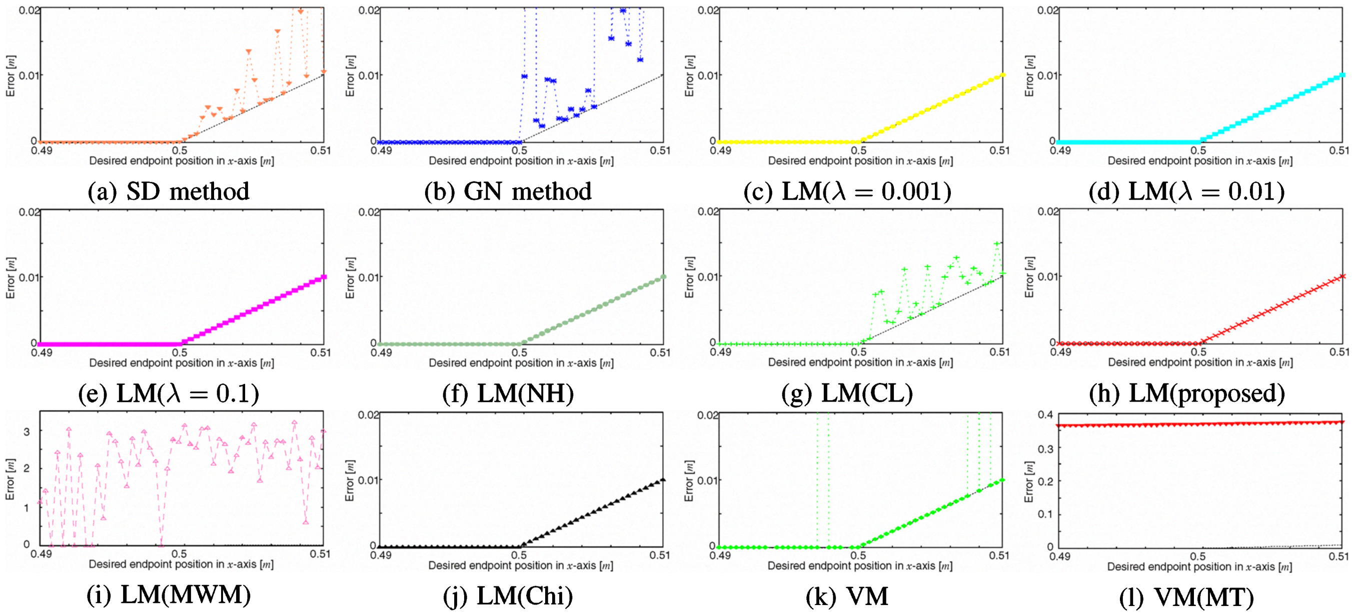

Fig. 5. Error comparison between SD, GN, LM(λ =const.), LM(NH), LM(CL), LM(proposed), LM(MWM), LM(Chi), VM and VM(MT) near the boundary of the solvable range. While LM(CL) showed unstable behavior, the proposed method succeeded in all cases. Although LM(λ =const.), LM(NH) and LM(Chi) showed successful results, they consumed long time for computations. See Fig.4.

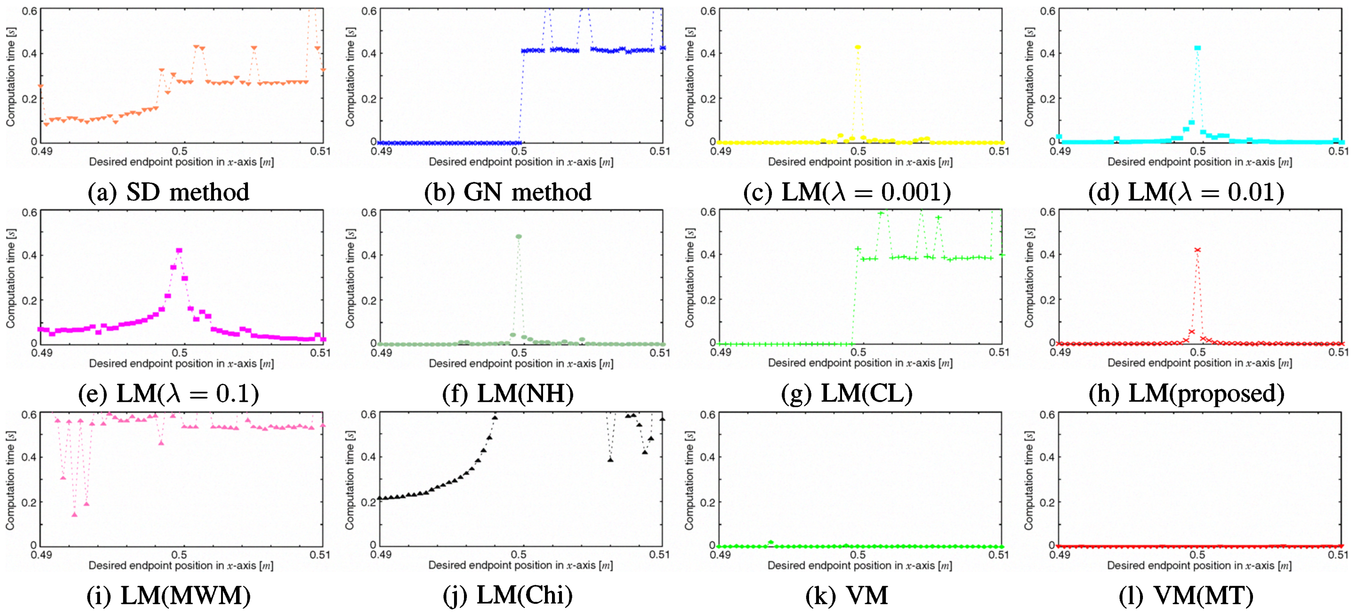

Fig. 6. Computation time comparison between SD, GN, LM(λ =const.), LM(NH), LM(CL), LM(proposed), LM(MWM), LM(Chi), VM and VM(MT) near the boundary of the solvable range. Though the proposed method took long time exactly at the boundary, the result was correct. Also, any other methods showed better performance than the proposed method.

robot's COM is about 0.29[m] at a standing posture, the planned COM trajectory passes unachievable range during the motion. Namely, IK frequently becomes unsolvable.

The points of interest in IK are listed in Table I with the weight on constraints. The total number of constraints is 30 and the degree-of-freedom of the robot is 18 (6 for the body and 6 for each leg), where the arm joints are not used in solving IK. Thus, it is basically an unsolvable problem even if the targeted COM height is set lower. The constraint on the vertical component of COM is rather loosened with a smaller weight than that on the horizontal components. Feet motions are designed by navigating four vertices, with smaller weights on the rear vertices on each sole.

Fig.7 shows snapshots of the synthesized motion. The COM and feet trajectories in vertical direction are plotted in Fig.8, in which COM height is automatically dragged down when the target COM is out of reach. Simultaneously, the feet trajectories are also automatically pulled up, which causes undesirably large acceleration. Fig.9 shows trajectories of knee joints, in which it is observed that they are stretched during the motion.

V. CONCLUSION

A simple but robust numerical IK solver based on LM was presented. It will be a fundamental tool to facilitate easy designs of a variety of motion particularly by non-specialists of robotics, since they don't need to pay attention to the solvability in addition to the singularity and redundancy. The author thinks the humanoid robot is one of the most relevant application of this technique.

The proposed method is basically concerned with the algebraic equation, and motion continuity is not taken into

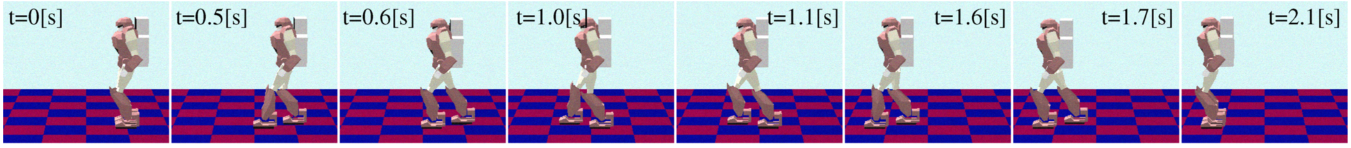

Fig. 7. Snapshots of a stretched-knee walk generated by the proposed IK technique.

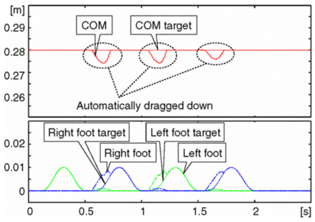

Fig. 8. COM and feet trajectory of the stretched-knee walk in vertical direction. The COM height was automatically dragged down.

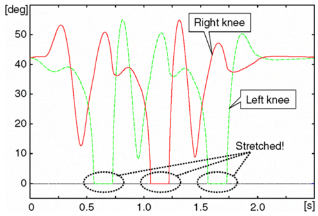

Fig. 9. Both left and right knee joint trajectories of the stretched-knee walk. IK computation didn't require any exceptional procedure.

account. The resulted stretched-knee walking motion in the previous section is not satisfactorily applicable to the real robot. An adaptive adjustment of the weights on constraints should be developed for physicallly feasible motion designs, which is the future work.

Appendix: Angle-Axis Vector

Let us define the following vector:

$$\boldsymbol{l} \equiv \begin{bmatrix} r_{32} - r_{23} \\ r_{13} - r_{31} \\ r_{21} - r_{12} \end{bmatrix} \tag{24}$$

for $\boldsymbol{R} = \{r_{ij}\}(i = 1 \sim 3, j = 1 \sim 3)$. If $\boldsymbol{R}$ is not diagonal, $\boldsymbol{l}$ should have non-zero length, and the angle-axis vector $\boldsymbol{a}$ which is equivalent with $\boldsymbol{R}$ is computed as follows:

$$\boldsymbol{a}(\boldsymbol{R}) \equiv \frac{\operatorname{atan2}(\|\boldsymbol{l}\|, r_{11} + r_{22} + r_{33} - 1)}{\|\boldsymbol{l}\|}\boldsymbol{l}. \tag{25}$$

If $\boldsymbol{R}$ is diagonal, four possibilities are $(r_{11}, r_{22}, r_{33}) = (1,1,1), (1,-1,-1), (-1,1,-1), (-1,-1,1)$. If two of (r_{11}, r_{22}, r_{33}) are -1, $\boldsymbol{a}$ is defined as follows:

$$\boldsymbol{a} \equiv \frac{\pi}{2}\begin{bmatrix} r_{11} + 1 \\ r_{22} + 1 \\ r_{33} + 1 \end{bmatrix}. \tag{26}$$

If $(r_{11}, r_{22}, r_{33}) = (1,1,1)$, $\boldsymbol{a} \equiv \boldsymbol{0}$.

Although Luh et al.[25] proposed to evaluate the orientational error by $\boldsymbol{l}$ in Eq.(24) instead of $\boldsymbol{a}$, it is not correct since it cannot distinguish four singular cases.

References

[1] D. L. Pieper, "The Kinematics of Manipulators under Computer Control," Ph.D. dissertation, Stanford University, 1968.

[2] M. Raghavan and B. Roth, "Kinematic Analysis of the 6R Manipulator of General Geometry," in *Proceedings of The Fifth International Symposium on Robotics Research*, 1991, pp. 263–269.

[3] D. E. Whitney, "The Mathematics of Coordinated Control of Prosthetic Arms and Manipulators," *Transactions of the ASME, Journal of Dynamic Systems, Measurement, and Control*, vol. 94, no. 4, pp. 303–309, 1972.

[4] J. Baillieul, "Kinematic Programming Alternatives for Redundant Manipulators," in *Proceedings of the 1985 IEEE International Conference on Robotics & Automation*, 1985, pp. 722–728.

[5] Y. Nakamura and H. Hanafusa, "Inverse Kinematic Solutions with Singularity Robustness for Robot Manipulator Control," *Journal of Dynamic Systems, Measurement, and Control*, vol. 108, pp. 163–171, 1986.

[6] C. W. Wampler, "Manipulator Inverse Kinematic Solutions Based on Vector Formulations and Damped Least-Squares Methods," *IEEE Transactions on Systems, Man, and Cybernetics*, vol. SMC-16, no. 1, pp. 93–101, 1986.

[7] D. N. Nenchev, Y. Tsumaki, and M. Uchiyama, "Singularity-Consistent Behavior of Telerobots: Theory and Experiments," *The International Journal of Robotics Research*, vol. 17, no. 2, pp. 138–152, 1998.

[8] D. W. Marquardt, "An Algorithm for Least-Squares Estimation of Nonlinear Parameters," *Journal of the Society for Industrial and Applied Mathematics*, vol. 11, no. 2, pp. 431–441, 1963.

[9] Y. Nakamura and K. Yamane, "Dynamics Computation of Structure-Varying Kinematic Chains and Its Application to Human Figures," *IEEE Transactions on Robotics and Automation*, vol. 16, no. 2, pp. 124–134, 2000.

[10] W. A. Wolovich and H. Elliot, "A Computational Technique for Inverse Kinematics," in *Proceedings of the 23rd IEEE conference on Decision and Control*, 1984, pp. 1359–1363.

[11] A. Balestrino, G. de Maria, and L. Sciavicco, "Robust Control of Robotic Manipulators," in *Proceedings of the 9th IFAC World Congress*, vol. 5, 1984, pp. 2435–2440.

[12] J. Zhao and N. I. Badler, "Inverse Kinematics Positioning Using Nonlinear Programming for Highly Articulated Figures," *ACM Transactions on Graphics*, vol. 13, no. 4, pp. 313–336, 1994.

[13] S. K. Chan and P. D. Lawrence, "General Inverse Kinematics with the Error Damped Pseudoinverse," in *Proceedings of IEEE International Conference on Robotics and Automation*, 1988, pp. 834–839.

[14] S. Chiaverini, "Estimate of the Two Smallest Singular Values of the Jacobian Matrix: Applications to Damped Least-Squares Inverse Kinematics," *Journal of Robotic Systems*, pp. 991–1008, 1988.

[15] R. V. Mayorga, N. Milano, and A. K. C. Wong, "A Simple Bound for the Appropriate Pseudoinverse Perturbation of Robot Manipulators," in *Proceedings of IEEE International Conference on Advanced Robotics*, 1991, pp. 1485–1488.

[16] A. S. Deo and I. D. Walker, "Robot Subtask Performance with Singularity Robustness Using Optimal Damped Least Squares," in *Proceedings of IEEE International Conference on Robotics and Automation*, 1992, pp. 434–441.

[17] E. D. Pohl and H. Lipkin, "A New Method of Robotic Motion Control Near Singularities," in *Proceedings of the Fifth IEEE International Conference on Advanced Robotics*, 1991, pp. 405–410.

[18] K. A. O'Neil, Y.-C. Chen, and J. Seng, "Removing Singularities of Resolved Motion Rate Control of Mechanisms, Including Self-Motion," *IEEE Transactions on Robotics and Automation*, vol. 13, no. 5, pp. 741–751, 1997.

[19] A. Hourtash, "The Kinematic Hessian and Higher Derivatives," in *Proceedings of the 2005 IEEE International Symposium on Computational Intelligence in Robotics and Automation*, 2005, pp. 169–174.

[20] G. H. Golub, P. C. Hansen, and D. P. O'Leary, "Tikhonov Regularization and Total Least Squares," *SIAM Journal of Matrix Analysis and Applications*, vol. 21, no. 1, pp. 185–194, 1999.

[21] N. Yamashita and M. Fukushima, "On the rate of convergence of the Levenberg-Marquardt method," Department of Applied Mathematics and Physics, Kyoto University, Tech. Rep. 2000-008, 2000.

[22] J. J. Moré and D. J. Thuente, "Line Search Algorithms with Guaranteed Sufficient Decrease," *ACM Transactions on Mathematical Software*, vol. 20, no. 3, pp. 286–307, 1994.

[23] T. Sugihara, K. Yamamoto, and Y. Nakamura, "Hardware design of high performance miniature anthropomorphic robots," *Robotics and Autonomous System*, vol. 56, pp. 82–94, 2007.

[24] T. Sugihara and Y. Nakamura, "Boundary Condition Relaxation Method for Stepwise Pedipulation Planning of Biped Robots," *IEEE Transaction on Robotcs*, vol. 25, no. 3, pp. 658–669, 2009.

[25] J. Y. S. Luh, M. W. Walker, and R. P. C. Paul, "Resolved Acceleration Control of Mechanical Manipulators," *IEEE Transactions on Automatic Control*, vol. AC-25, no. 3, pp. 468–474, 1980.